



ISSN 1349-1113  
JAXA-RR-09-002E

## JAXA Research and Development Report

---

# **Improvement of viscosity measurements using oscillation drop techniques with electrostatic levitators**

Takehiko ISHIKAWA, Jumpei-T OKADA,  
Paul-François PARADIS and Yuki WATANABE

February 2010

Japan Aerospace Exploration Agency

# Improvement of viscosity measurements using oscillation drop techniques with electrostatic levitators

By

Takehiko ISHIKAWA<sup>1</sup>, Jumpei-T OKADA<sup>1</sup>,  
Paul-François Paradis<sup>1</sup> and Yuki WATANABE<sup>2</sup>

## ABSTRACT

Electrostatic levitators use strong electric fields to levitate and accurately position a sample against gravity. In this study, the effects of the electric field are investigated with regards to viscosity measurements conducted with the oscillating drop method. The effects of the external field on viscosity measurements are experimentally confirmed by changing the sample size. Moreover, a numerical simulation based on a simple mass-spring-damper system can reproduce the experimentally observed effects. Based on the above results, measurement procedures were improved. These help to minimize the effect of the positioning force and increase the accuracy of the viscosity measurements.

## 1. Introduction

To improve the accuracy of computer simulations for material processing such as casting and crystal growth, the knowledge of thermophysical properties of high temperature metals and alloys is paramount<sup>1</sup>. Due to their high melting temperature and the risk of chemical reactions between samples and crucibles, property measurements of high temperature melts are very difficult to perform with conventional methods. Non-contact techniques have been widely used for property determination of high temperature materials to solve the above mentioned problems. So far, density, heat capacity, surface tension, viscosity, total hemispherical emissivity, thermal conductivity, and electrical resistivity have been measured with a variety of techniques that includes aerodynamic<sup>2,3</sup>, electromagnetic<sup>4-6</sup>, and electrostatic<sup>7-10</sup> levitation.

Among those properties, the viscosity is one of the most important for numerical simulations since it corresponds to atomic mobility in the melt<sup>11</sup>. However, the number of viscosity reported data is smaller than that of other properties (e.g., density, surface tension), in particular for refractory metals and alloys. Therefore, measurements with a containerless technique are highly desired.

When levitators are used, the viscosity is usually measured by the oscillating drop technique<sup>10,12</sup>. In this method, a levitated drop is first intentionally deformed from its spherical shape by applying an external force. When the force is removed, the sample shape goes back to the original spherical shape through oscillatory shape changes. The viscosity can then be obtained from the decay time needed to restore the original shape. This oscillating drop technique assumes the following three conditions: (a) the liquid sample is spherical before the induced oscillation; (b) the internal flow in the sample is laminar<sup>13</sup>; and (c) the levitated droplet is free from any external forces.

It is very difficult to satisfy these conditions with current levitation systems due to gravity. For electromagnetic levitation, which is currently the most widely used technique, large electric currents are induced in the sample in order to levitate it against

---

1 Japan Aerospace Exploration Agency, 2-1-1 Sengen, Tsukuba, Ibaraki, Japan 305-8505.

2 Advanced Engineering Services Co. Ltd., 1-6-1 Takezono, Tsukuba, Ibaraki, Japan 305-0032

gravity. By doing so, it adopts a non-spherical shape. Moreover, a turbulent flow is induced inside the droplet and the melt is always vibrating even if no force to trigger oscillations is intentionally applied. This explains why viscosity measurements with electromagnetic levitator are currently conducted under reduced gravity conditions<sup>12)</sup>.

Electrostatic levitators satisfy the above required conditions of sample sphericity and laminar flow even under normal gravity condition, and allow viscosity measurements of high temperature melts. So far, measurements for refractory metals<sup>14,15)</sup>, semiconductors<sup>16,17)</sup>, glass forming alloys<sup>18,19)</sup>, and oxide materials<sup>20)</sup> have been reported. However, even with this technique, the levitated sample is not free from external forces. In order to levitate a sample of mass  $m$  with surface charge  $Q$  against a gravitational acceleration  $g$ , a large electric field  $E$  obeying the following equation is necessary:

$$E = \frac{mg}{Q} \quad (1)$$

In general, an electric field in the 5 to 10 kV/m range is necessary to levitate a sample which weighs around 20 mg with a surface charge of around  $10^{-10}$  C. In addition, since a three-dimensional electrostatic potential minimum does not exist (Earnshaw's theorem), sample positioning is only possible if an actively controlled electric field is used<sup>22)</sup>. Therefore, viscosity measurements with these levitators are conducted under strong electric fields with DC and AC components.

This implies that all reported viscosity values measured so far by electrostatic levitators contain a certain amount of errors due to the electric field. However, the effect of the electric field on the viscosity measurements in electrostatic levitators has not been investigated yet. Viscosity measurement technique using electrostatic levitation and oscillating drop was developed by Rhim *et al.*<sup>9)</sup> Although a detailed measurement procedure is given in ref. 9, nothing is mentioned about this effect. Hyers<sup>22)</sup> pointed out that the positioning field would change the measured damping of the surface oscillations, but reported no experimental evidence.

In this study, to change the magnitude of the electric field, zirconium samples of different sizes were levitated, melted, and kept at their melting temperature before performing viscosity measurements with the oscillating drop method. Moreover, levitation control parameters such as proportional-differential-integral (PID) values and frequency of the feedback control were changed and their effects on viscosity were also examined. The experimental results were compared with a simple simulation based on the mass-spring-damper system, and the effect of electric field was quantitatively evaluated. Based on these results, a procedure to reduce the effect of the positioning electric field on viscosity measurements was proposed and experimentally confirmed.

This paper first describes the electrostatic levitation system and the viscosity measurement method, and then presents the results of both experiments and simulations.

## 2. Experiment setup

### 2.1 Electrostatic levitator

The electrostatic levitation system used in our laboratory is similar to the one developed by Rhim *et al.*<sup>21)</sup> but includes several modifications. A detailed description of the facility is given elsewhere.<sup>15)</sup> Fig. 1 depicts schematically the apparatus. It consisted of a stainless steel chamber that was evacuated to a pressure of around  $10^{-5}$  Pa. The chamber housed a pair of parallel disk electrodes, typically 10 mm apart between which a positively charged sample was levitated. The top electrode was kept electrically negative. These electrodes were utilized to control the vertical position ( $z$ ) of the specimen. The typical sample size was 2 mm in diameter. In addition, four spherical electrodes distributed around the bottom electrode were used for horizontal control ( $x$  and  $y$ ). The lower electrode was surrounded by four coils that generated a rotating magnetic field which were used to control sample rotation<sup>10)</sup>.

Sample heating was achieved using two 100 W CO<sub>2</sub> lasers. One laser beam was sent directly to the sample whereas the other beam was divided into two portions such that three focused beams, separated by 120 degrees in a horizontal plane, hit the sample. This multiple beam configuration minimized the laser induced disturbances along the horizontal. The position stability was around 200  $\mu$ m along the vertical axis and 100  $\mu$ m along the horizontal axis<sup>23)</sup> The sample temperature data were obtained using single-color pyrometers.

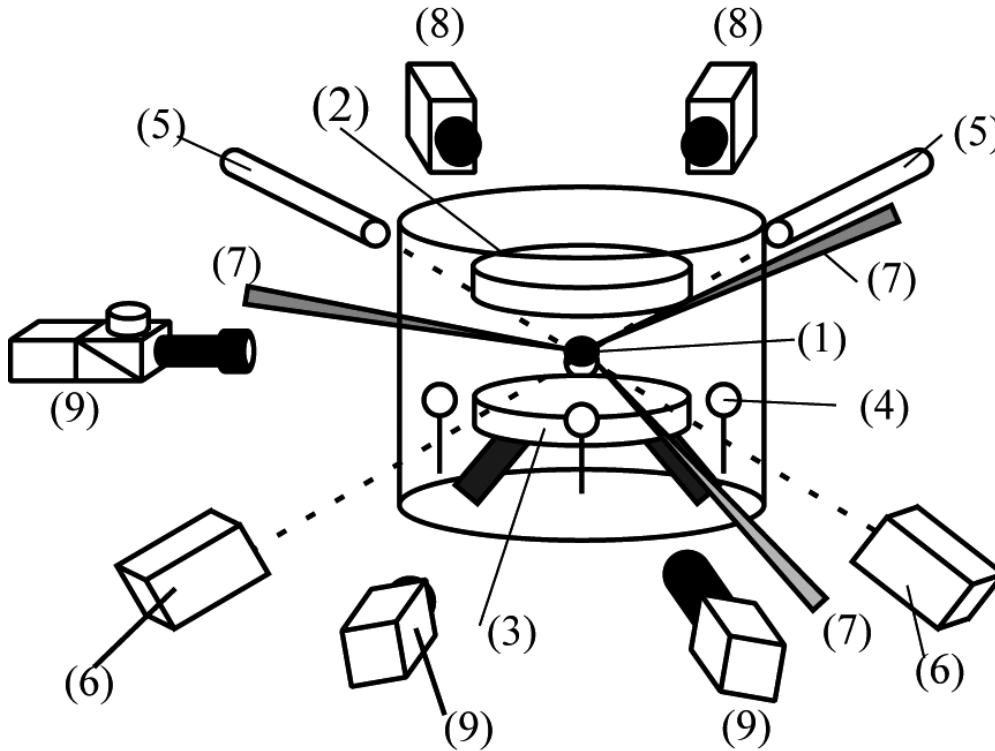


Fig.1 Schematic view of the electrostatic levitation furnace and its diagnostic apparatus: (1)sample, (2) top electrode, (3) bottom electrode, (4) side electrode, (5) He-Ne laser, (6) position detector, (7) CO<sub>2</sub> laser beam, (8) pyrometer, and (9) CCD cameras.

The sample was observed by three charged-coupled-device cameras. One camera offered a view of both the electrode assembly and the sample. In addition, two black and white high-resolution cameras (60 Hz sampling rate), located at right angle from each other and equipped with telephoto objectives in conjunction with background lamps, provided magnified views of the sample. The recorded images were used to measure the radius of the sample from which the density was obtained.

The active feedback position control system consisted of position sensing, PID calculation, and variation of the electric field. Position sensing was achieved with a set of orthogonally disposed He-Ne laser that projected a sample image on position sensors. One sensor detected the y-z position whereas another sensor was dedicated to the x position. Fig. 2 illustrates the hardware arrangement for position control. The beam of a He-Ne laser was expanded and impinged on a levitated sample. The size of the resulting sample shadow was optimized with a lens to cover the area of the sensor such that a good dynamic range was obtained. In addition, a polarization filter was used to optimize the laser intensity reaching the position sensing device (PSD)(Hamamatsu C7339). The PSD was equipped with a band-pass filter to eliminate the photon noise coming from sources other than the laser. The sample position signals read by the PSD were then fed to a computer through an interface board (National Instruments PC-MIO-16 XE-50) where analogue to digital conversion took place. The measured current positions were compared with preset positions by a computer and control signals (voltages for electrodes) were generated according to the PID servo algorithm. The z-direction control voltage at the i-th cycle  $V_{zi}$  was determined by the following formula:

$$V_{zi} = P_z \times \varepsilon_i + I_z \times \sum_{j=0}^i \varepsilon_j + D_z \times (\varepsilon_i - \varepsilon_{i-1}), \quad (2)$$

where  $\varepsilon_i$  is the difference between the current and the aimed positions, and  $P_z$ ,  $D_z$ , and  $I_z$  are respectively the proportional, derivative, and integral gains. Similar controls were applied to the horizontal directions (x and y) without the integral term. These PID parameters could be changed at will during sample levitation. Also, the vertical feedback control rate could be selected as 720 Hz or 240 Hz. The control rate for the horizontal direction (x and y) was fixed to 30 Hz.

## 2.2 Viscosity measurement system

An isolated liquid drop, free from external forces, adopts a spherical shape due to the uniform surface tension. If the drop undergoes a small amplitude axi-symmetric oscillation, the drop shape  $r(t)$ , in the weak damping limit, can be described by:

$$r(t) = r_0 + \sum_{n=2}^{\infty} r_n \cos(\omega_n t) P_n(\cos \theta) \exp\left(\frac{-t}{\tau}\right) \quad (3)$$

where  $r_0$  is the radius of the drop when it assumes a spherical shape,  $P_n(\cos \theta)$  is the  $n$ th order Legendre polynomial, with  $\theta$  being the angle measured between the  $z$  axis and the radial direction, and  $r_n$  is the oscillation amplitude of the  $n$ th mode. The characteristic oscillation frequency  $\omega_n$  corresponding to the  $n$ th mode is expressed by:<sup>24)</sup>

$$\omega_n^2 = n(n-1)(n+2) \frac{\gamma}{\rho r_0^3}, \quad (4)$$

where  $\gamma$  is the surface tension and  $\rho$  is the density of the drop. The damping constant  $\tau_n$  in eq. (3) can be found by:<sup>25)</sup>

$$\frac{1}{\tau_n} = (n-1)(2n+1) \frac{\eta}{\rho r_0^2} \quad (5)$$

where  $\eta$  is the viscosity of the liquid sample. For  $n = 2$ , the drop shows axi-symmetric oscillations at the frequency

$$\omega_2^2 = \frac{8\gamma}{\rho r_0^3} \quad (6)$$

and the oscillation decay with the time constant

$$\frac{1}{\tau_2} = \frac{5\eta}{\rho r_0^2} \quad (7)$$

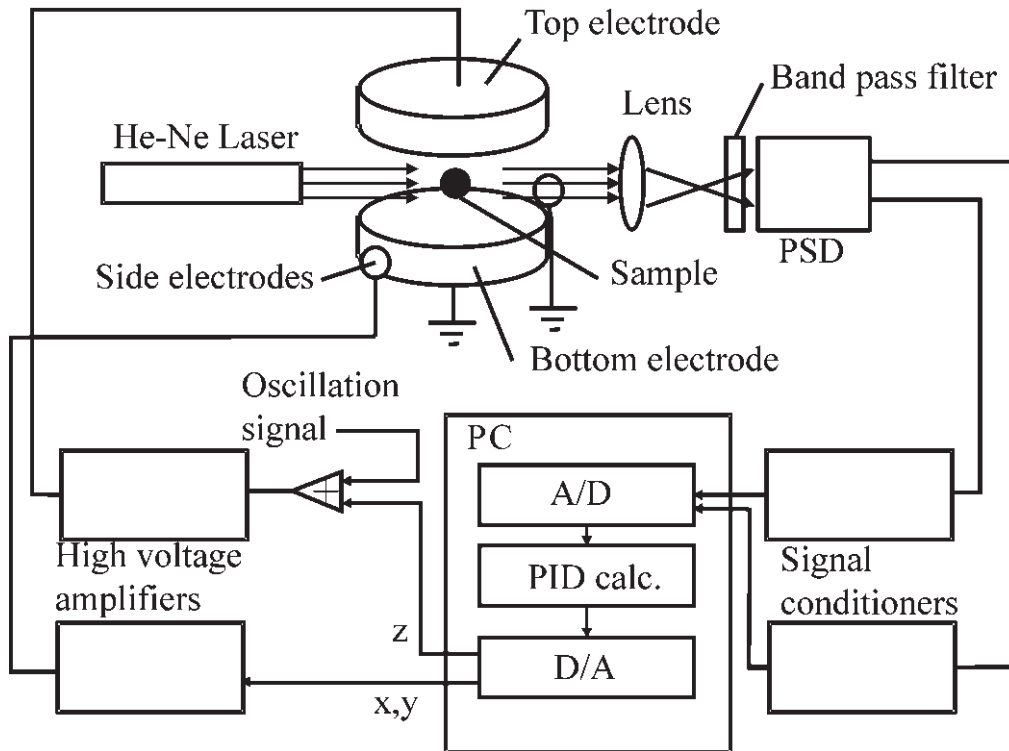


Fig.2 Schematic diagram of the sample position control system.

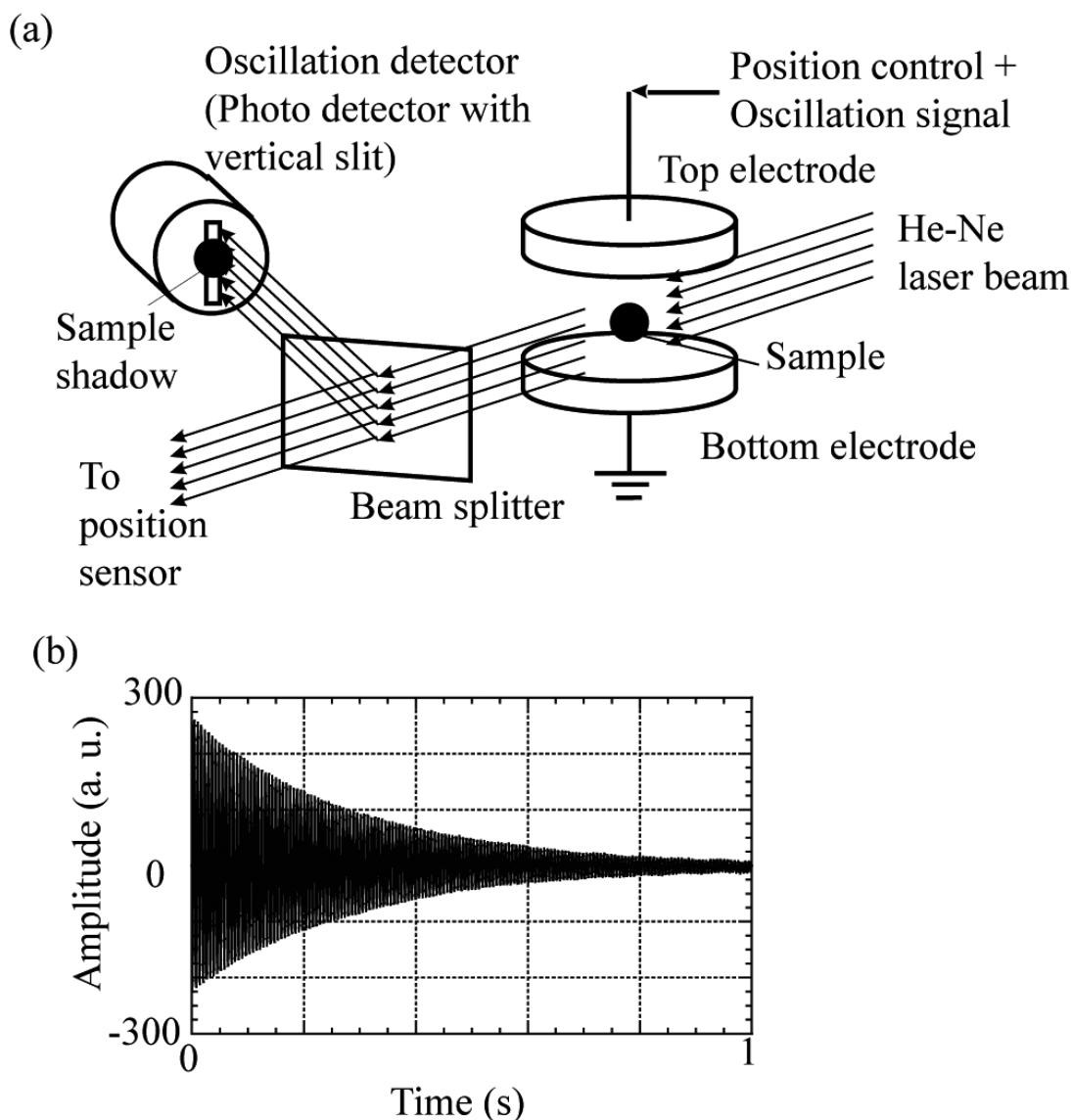


Fig.3 Sample oscillation detection for surface tension and viscosity measurements: (a) diameter sensing system and (b) decay of the signal of the oscillation following electrical excitation for a molten sample measured by the sensing system.

In the experiments, a sample was molten and kept at a selected temperature. During the sample heating, electric currents were applied to four coils to rotate the sample about the vertical axis at a rate of around 5 Hz. This amount of sample rotation stabilized the rotation axis and helped eliminate the measurement error due to the random rotation of the sample. The rotating magnetic field was then removed before viscosity measurements were carried out. The 2<sup>nd</sup> mode of drop oscillation was induced to the sample by superimposing on the levitation field a small sinusoidal electric field with a frequency given by eq. (6). An oscillation detection system, illustrated in Fig. 3(a), measured the fluctuation of the vertical diameter of the molten sample with a 4096 Hz sampling frequency. The typical transient signal that followed the termination of the excitation field is shown in Fig.3(b). This signal was analyzed by a custom-made LabVIEW<sup>TM</sup> program (based on ref. 9) and the time constant  $\tau_2$  was determined. This was done several times for a given temperature. The radius of the sample  $r_0$  was obtained from the image analysis and the data of the liquid density  $\rho$  could be found<sup>7)</sup>. Knowing these quantities, the viscosity could be calculated from eq. (7).

### 3. Experiments and simulations

#### 3.1 Experiment 1 and 2

To evaluate the effects of the levitation force on viscosity, experiments with zirconium samples of different sizes were conducted. Among refractory metals, zirconium was chosen because of its easiness to levitate and melt (melting point: 2128 K), its low vapor pressure (provides good position stability), and the availability of literature values. The samples were prepared by cutting a zirconium wire (99.9 mass % purity) into pieces and then arc melting them into spheroids. The sample mass ranged from around 10 mg to 80 mg. All samples were levitated one at the time, melted, and kept at the melting temperature. Then, sample oscillations were induced and the decay time was measured. The measurements were repeated several times for each sample. The first series of measurements (experiment-1), listed in Table-1, were conducted with the following control parameters:  $P_z = 2.4 \times 10^6$  V/m,  $I_z = 1.23 \times 10^5$  V/ms,  $D_z = 1.25 \times 10^4$  Vs/m, and feedback control frequency of 720 Hz. Until now, these control parameters have been used as a standard for thermophysical property measurements of refractory metals. As shown in Table-1, a larger electric field is necessary to levitate larger samples. Fig. 4 illustrates the measured viscosity as a function of sample mass. When the samples were small, the measured values were within the range of literature data listed in Table-2<sup>9,14,26,27</sup>) and appearing in Fig. 4. When the sample became larger, the measured viscosity increased and deviated from the literature values. For the 80 mg sample, the measured values were almost 3.3 times larger than the literature data. Fig. 5 shows the decay time ( $\tau_2$ ) versus sample mass. According to eq. (7),  $\tau_2$  should increase when the mass became larger. However,  $\tau_2$  became smaller when the mass was larger than 40 mg and converged to a constant value of 0.23 s. If  $\tau_2$  is constant, the viscosity value is proportional to the square of the sample radius, explaining the steep increase of viscosity in Fig. 4. Similar experiments were conducted with different metals (Sn, Si, Nb) and an alloy (Ni-Zr). All of these samples exhibited the same tendency for the mass and viscosity relation.

Table-1 Experimental results of viscosity measurements for different Zr samples at the melting temperature. Control parameters for vertical direction were  $P_z = 2.4 \times 10^6$  V/m,  $I_z = 1.23 \times 10^5$  V/ms,  $D_z = 1.25 \times 10^4$  Vs/m, with a feedback control frequency of 720 Hz.

Sample Mass (mg)	Oscillation frequency (Hz)	Electric field (kV/cm)	Viscosity (mPa.s)		
			Number of data	Averagevalue	Standard deviation
16.4	275	8.2	14	2.98	0.27
17.5	263	8.4	31	3.20	0.36
27.6	207	9.3	16	3.48	0.13
34.8	188	9.8	36	3.49	0.68
35.1	180	9.7	27	3.59	0.96
35.8	182	9.7	26	4.26	0.45
40.0	174	10.6	38	5.72	1.31
42.7	167	10.7	39	6.46	0.55
53.8	146	10.7	51	7.81	1.23
59.9	144	11.3	55	7.52	1.83
71.8	126	11.2	20	10.53	0.70
81.0	120	11.8	53	12.96	0.80
85.4	116	12.1	36	11.79	1.15

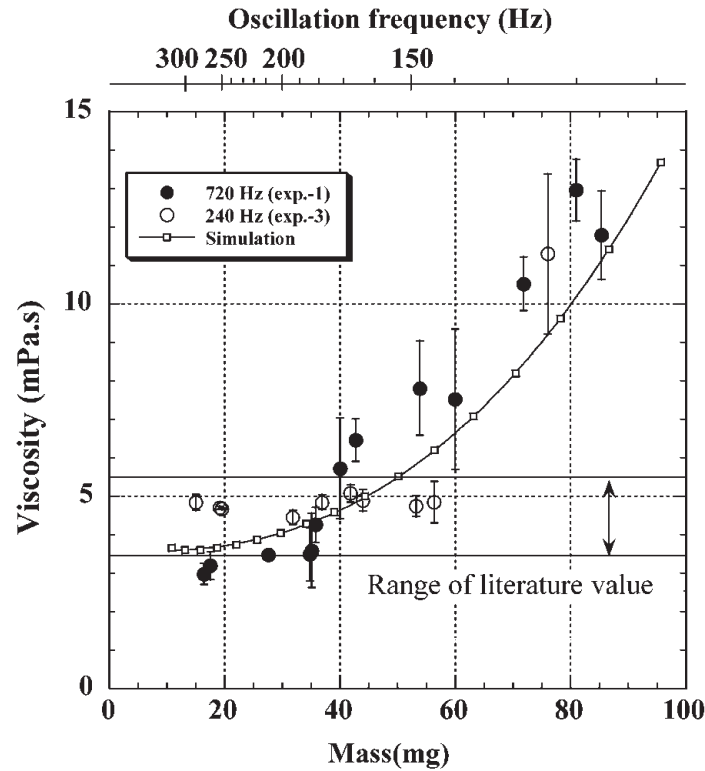


Fig.4 Measured and simulated viscosities versus sample mass. Black and white circles represent respectively the data measured for samples levitated with vertical feedback frequencies of 720 Hz and 240 Hz. White squares with the solid line show the simulation results described in section 3.2.

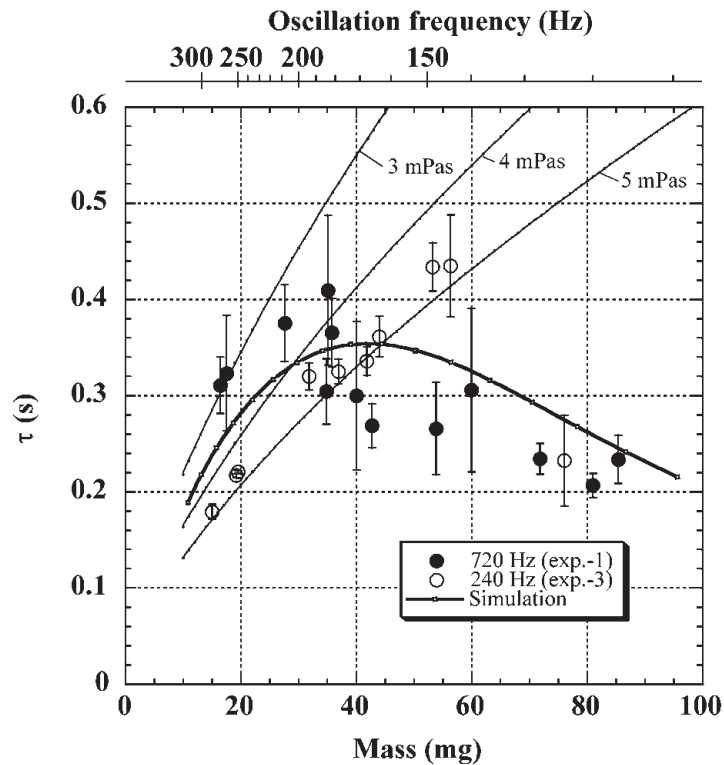


Fig.5 Measured and simulated decay time ( $\tau_2$ ) versus sample mass. Black and white circles respectively represent the data measured for samples levitated with vertical feedback frequencies of 720 Hz and 240 Hz. White squares with the solid line show the simulation results described in section 3.2. Ideal mass versus  $\tau_2$  lines for viscosity values of 3, 4, and 5 mPa.s are also plotted for reference.

Table-2 Literature values for the viscosity of molten zirconium at the melting temperature.

Viscosity (mPa.s)	Uncertainty	Method	Reference
3.5		Capillary	26) thorough 28)
5.45		Capillary	27) thorough 29)
4.86	6%	Levitation	9)
4.83		Levitation	14)

Three causes were thought to explain this phenomenon. The first and the second causes were the effect of flow (turbulent and laminar) inside the sample. As for the turbulent flow, it was previously reported that the viscosity measured with an electromagnetic levitator in microgravity was 13 times larger than the literature values due to the turbulent flow inside the sample<sup>13)</sup>. However, based on an analysis by Hyers<sup>22)</sup>, the internal flow in the electrostatically levitated drop was laminar even under terrestrial conditions, and the calculated Reynolds number was much smaller than the critical number for turbulence. Therefore, turbulent flow could not be the cause of observed phenomenon.

Ref. 22 also pointed out that laminar flow might also lead to self-excited oscillations, especially for electrostatic levitation where thermo-capillary convection is important. This possibility could not be evaluated at this moment. The third possible cause was the interaction between the position control force and the sample oscillation, which was also pointed out in ref. 22.

The second series of measurements (experiment-2) was conducted to investigate the effect of position control on viscosity. In these measurements, a zirconium sample (51.7 mg) was levitated, melted, and kept at the melting temperature. Then, drop oscillations (155 Hz) were induced with a variety of controlled parameters (PID control gains and feedback control frequencies), as listed in Table-3.

By comparing the results of experiments 2-1 and 2-3 in Table-3, the higher PID parameters resulted in the higher measured viscosity. For experiments 2-2 and 2-4, two Bessel low pass filters (with 144 Hz cut-off frequency) were inserted between the D/A converter and the high voltage amplifier. This lowered the amplitude of the AC component of the electric field around the oscillation frequency. The results showed that these filters lowered the measured values, indicating that the oscillation damping was sensitive to the magnitude of the electric field. When the control frequency was reduced from 720 to 240 Hz, the measured viscosity was lowered to 4.9 mPa.s, which was within the range of the literature values. The results of experiment-2 clearly showed that the oscillation damping was seriously affected by the sample position control. In addition, since all experiments were conducted with the same sample, heating configuration, and temperature, the internal flow in the sample can be considered as constant throughout experiment-2. Judging by the fact that the oscillation damping was drastically changed by varying the position control parameters under constant internal flow condition, it can be concluded that the interaction between the sample position control and the sample oscillation is the main reason for the phenomenon observed in experiment-1.

Table-3 Position Control Parameters and measured viscosity for a 51.7 mg zirconium sample. The sample oscillation frequency was 155 Hz.

Exp.number	Control Frequency (Hz)	PID Gains			Low pass filter	Averaged measured viscosity (mPa.s)
		P <sub>z</sub> (10 <sup>6</sup> V/m)	D <sub>z</sub> (10 <sup>4</sup> Vs/m)	I <sub>z</sub> (10 <sup>5</sup> V/ms)		
2-1	720	2.6	1.4	1.23	No	15.4
2-2	720	2.6	1.4	1.23	YES	8.6
2-3	720	1.3	0.6	1.23	No	10.8
2-4	720	1.3	0.6	1.23	YES	6.8
2-5	240	1.3	1.7	1.23	No	4.9
2-6	240	1.3	1.7	1.23	YES	Could not levitate

### 3.2 Numerical simulations

A simple simulation was conducted to theoretically understand the interaction between the sample position control and the oscillation damping, and its impact on viscosity measurement. A simple system consisting of a mass, a spring, and a damper (Fig.6) was used as an analog of an oscillating drop. In this system, the spring (constant  $k$ ), the damper (constant  $c$ ), and the displacement ( $\xi$ ) correspond respectively to the surface tension, the viscosity, and the fluctuation of the vertical radius of an oscillating droplet from its equilibrium radius.

The positioning force  $F$  is applied to the charged mass ( $m$ ) through an electrical field. This force is composed of AC components with a wide frequency range. When the levitated droplet oscillated with a characteristic frequency  $\omega_2$ , the center of gravity of the melt also made slight sinusoidal translation along the vertical direction with frequency  $\omega_2$ . This motion was detected by a PSD and the levitation force was adjusted via the PID control. The fluctuation of the levitation force  $\Delta F$  due to the oscillatory sample translation can be expressed as:

$$\Delta F = f(\omega_2) \cos(\omega_2 t + \phi) \quad (8)$$

where  $\omega_2$  is the resonance frequency of the mass-spring-damper system defined by

$$\omega_2 = \sqrt{\frac{k}{m}}, \quad (9)$$

$f(\omega)$  is the intensity of the force with frequency  $\omega$ , and  $\phi$  is the phase difference between  $\xi$  and  $\Delta F$ . Since  $F$  is the Coulomb force between the charged sample and the electrodes,  $f(\omega)$  can be expressed as:

$$f(\omega) = Q \cdot E \cdot G(\omega) = m \cdot g \cdot G(\omega) \quad (10)$$

where  $G(\omega)$  is the frequency spectrum of the electric field, which can be measured by a FFT analysis of the levitation voltage.

As described earlier, once the excitation voltage is removed, the sample oscillation is damped due to viscosity. The time evolution of  $\xi$  can be determined by the following equation:

$$m \xi'' = -c \xi' - k \xi + h(t) f(\omega_2) \cos(\omega_2 t + \phi). \quad (11)$$

The constants  $k$  and  $c$  can be calculated from the surface tension, the viscosity, and the sample radius as:

$$k = \frac{32\pi}{3} \gamma \quad (12)$$

$$c = \frac{40\pi}{3} r_0 \eta \quad (13)$$

The function  $h(t)$  expresses that the amplitude of  $\Delta F$  becomes smaller as the oscillation is damped, and the following function was used in this simulation:

$$h(t) = \exp(-\alpha t) \quad (14)$$

where

$$\alpha = c / 2m. \quad (15)$$

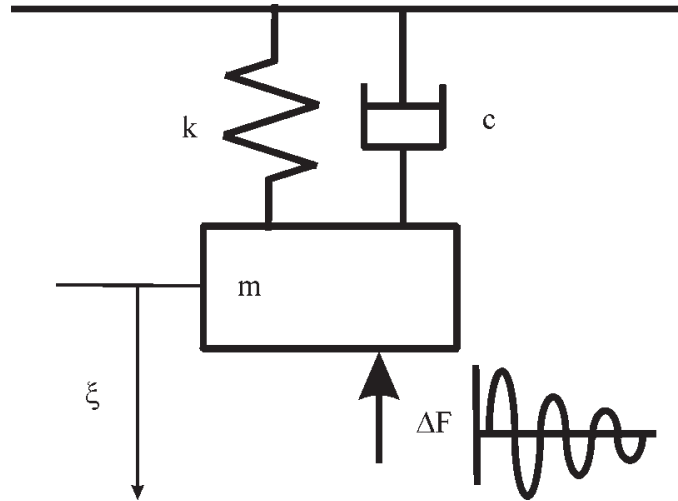


Fig.6 The mass, spring, and damper system used for numerical simulations.

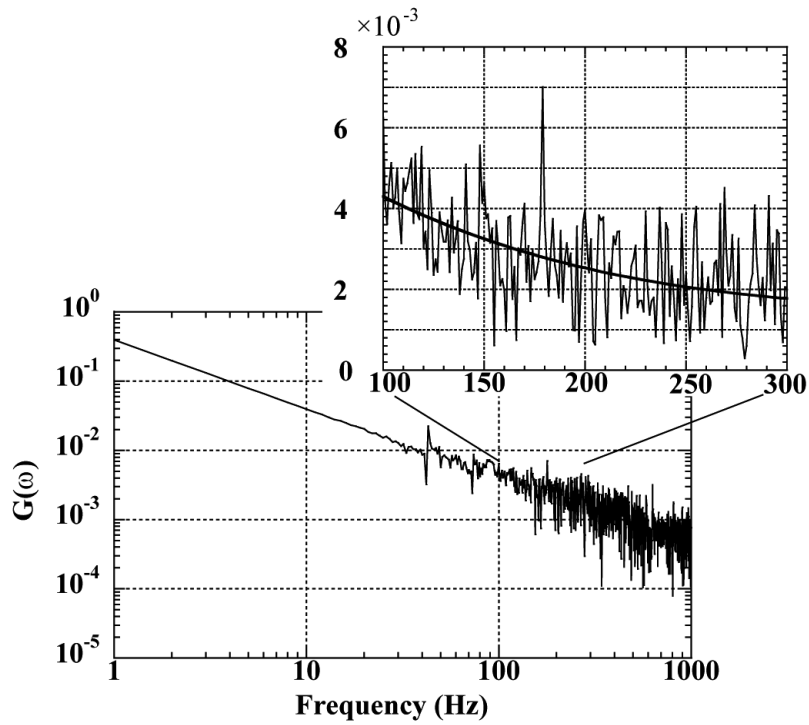


Fig.7 Measured frequency spectrum of the levitation electric field  $G(\omega)$ . The insert shows a magnified view of the frequency over the 100 to 300 Hz range.

Table-4 Parameters used for the simulation.

Density	6130 kg/m <sup>3</sup>
Viscosity	4 x10 <sup>-3</sup> Pa.s
Surface tension	1.5 N/m
Surface charge per area	2.3 x 10 <sup>-5</sup> C/m <sup>2</sup>
Initial displacement, $\xi(0)$	0.15 mm
Time step for calculation	10 <sup>-7</sup> s

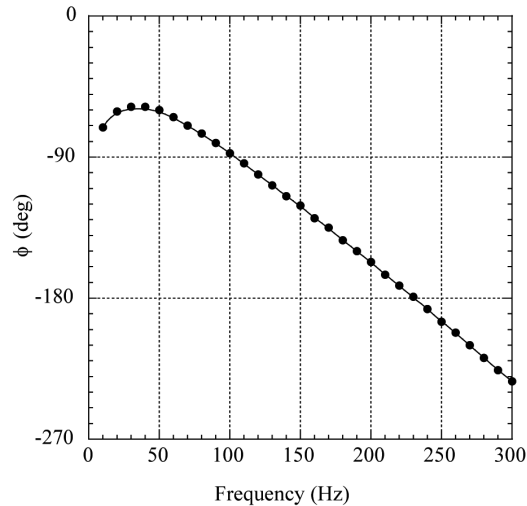


Fig.8 Measured phase  $\phi$  as a function of frequency.

$G(\omega)$  and  $\phi$  were actually measured using a FFT analyzer and a lock-in amplifier, as shown in Figs.7 and 8. The equation (11) was solved with a Runge-Kutta method<sup>30</sup>. The parameters used for the simulation are listed in Table-4. The initial displacement  $\zeta(0)$  was determined to be 0.15 mm by analyzing the image of an oscillating droplet.

Once  $\zeta(t)$  was computed, the simulated oscillation data were sent to the viscosity measurement program and both  $\tau_2$  and  $\eta$  could be calculated. The results of the simulation appear in Fig 4 and exhibit a good agreement with the experimental results.

### 3.3 Experiment-3 and 4

Results of both experiments-1, 2 and simulation indicated that the AC component of the positioning force at the characteristic frequency has made a significant interaction with the damping of the sample oscillation. One way to minimize this effect is to reduce the position control frequency. Fig.9 illustrates the concept. The oscillation frequency of the levitated sample ranges from around 100 Hz to 300Hz. Based on the sampling theory, position signals up to 360 Hz can be detected when the feedback control frequency is 720 Hz. Since the frequency range of the sample position overlapped with the sample oscillation frequency, the positioning force interferes with the sample oscillation.

If the feedback control frequency  $f_s$  is reduced to satisfy  $f_s/2 < \omega_2/2\pi$  (Fig. 9(b)) so that the positioning frequency range is separated from the sample oscillation frequency, the decay of the oscillation will not be affected by the positioning force. Viscosity measurements of zirconium samples with different sizes were conducted with a positioning feedback control frequency of 240 Hz. The results are listed in Table-5 and plotted in Fig. 4. The measured viscosity values became constant even if the sample mass changed from 10 mg to 56 mg. These results support the above hypothesis, and highlight the fact that it is important to adequately set the sample oscillation frequency out of the positioning feedback control frequency region to obtain accurate values of the viscosity.

When the sample size reached 76 mg, the frequency of oscillation (125 Hz) was close to that of the positioning control (120 Hz) and the viscosity measurements were affected. Moreover, when the feedback control frequency was set less than 180 Hz, stable levitation of molten samples became nearly impossible. These results suggested that there was a lower limit on the position control frequency for stable sample levitation. Moreover, this limited the maximum sample size whose viscosity could be measured without the effect of sample position control.

As for experiments-4, viscosity measurements with 240 Hz feedback control frequency were conducted for terbium (Tb) and niobium (Nb) samples. The results are shown in Fig.10 for Tb<sup>33</sup>) and in Fig.11 for Nb<sup>34</sup>). The viscosity measurements with 720 Hz frequency were also plotted in these figures. In the case of Tb (in which oscillation frequencies were around 180 Hz), the absolute viscosity values were strongly affected by the sample positioning control. For Nb (oscillation frequency near 240 Hz) the absolute

values were identical with both control frequencies. However, scatter of data with the 240 Hz control frequency was considerably smaller than that with 720 Hz.

Based on this research, the interaction between the position control and the sample oscillation was found to have a detrimental effect on viscosity measurements when an electrostatic levitation system is used. In order to minimize this impact, it is important to select the sample size and the position control parameters so that the control frequency will not overlap with the sample oscillation frequency.

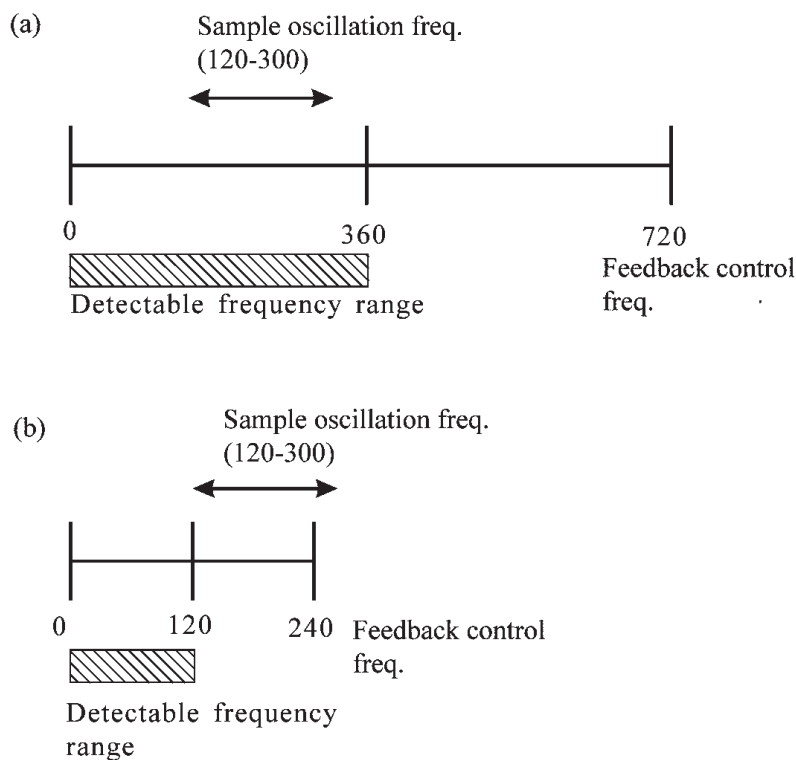


Fig.9 Conceptual drawing showing how to avoid the effect of sample positioning force in the viscosity measurement using the oscillating drop method: (a) current frequency relation between position control and sample oscillation with 720 Hz feedback control frequency, (b) relation when the feedback control frequency is reduced to 240 Hz.

Table-5 Experimental results for viscosity measurements of different Zr samples at the melting temperature. The control parameters for the vertical direction were  $P=1.3 \times 10^6$  V/m,  $I=1.23 \times 10^5$  V/ms,  $D=1.25 \times 10^4$  Vs/m, and the feedback control frequency was 240 Hz.

Sample Mass (mg)	Oscillation frequency (Hz)	Electric field (kV/cm)	Viscosity (mPa.s)		
			Number of data	Averagevalue	Standard deviation
15.0	289	7.9	7	4.84	0.2
19.2	258	9.1	13	4.70	0.04
19.5	255	9.1	10	4.67	0.02
31.8	197	10.1	11	4.45	0.19
36.9	183	10.3	11	4.84	0.19
41.8	171	10.3	14	5.07	0.22
44.0	166	10.4	11	4.89	0.28
53.2	150	10.6	14	4.74	0.27
56.3	146	10.9	13	4.85	0.54
76.0	125	11.3	15	11.3	2.08

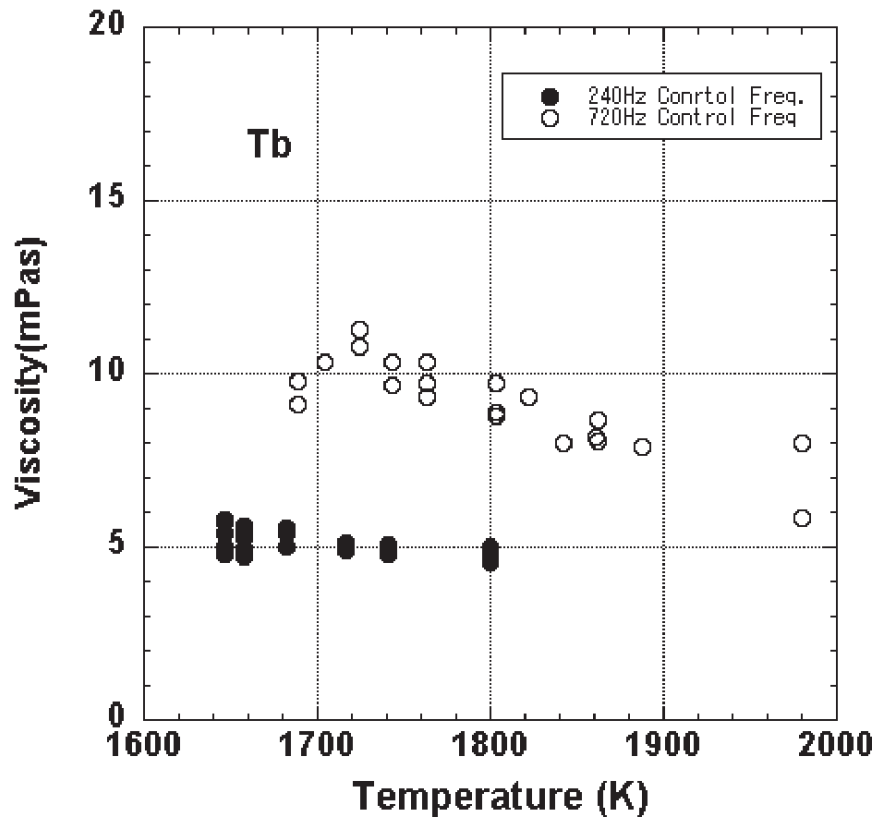


Fig.10 Viscosity of terbium vs temperature.

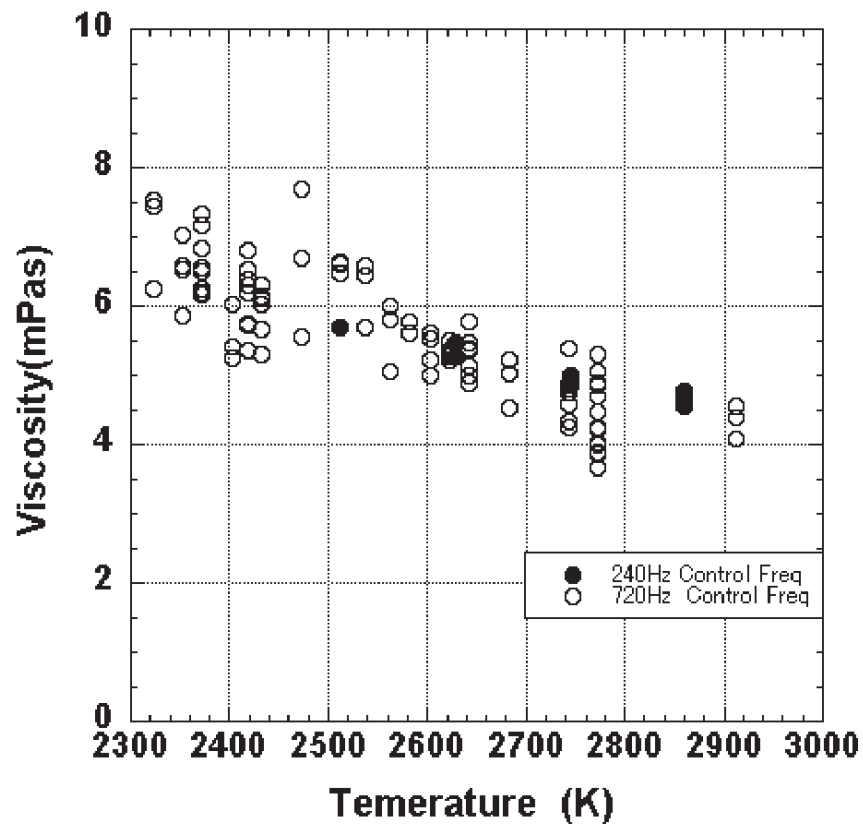


Fig.11 Viscosity of niobium vs temperature.

#### 4. Discussions

Whether the positioning force  $\Delta F$  enforces or suppresses the oscillation damping depends heavily on the phase  $\phi$ . When the drop oscillation is free from any external forces,  $\xi(t)$  (eq. (10)) can be solved with initial conditions  $\xi(0)=A$  and  $\xi'(0)=0$ , and, assuming  $\omega_2 \gg \alpha$ , such that:

$$\xi(t) = A \exp(-\alpha t) \cos \omega_2 t. \quad (16)$$

From eq. (16),  $\xi'(t)$  can be obtained as:

$$\xi'(t) = -A\omega_2 \exp(-\alpha t) \sin \omega_2 t, \quad (17)$$

and the damping term in eq. (11) can be rendered as:

$$-c\xi' = -cA\omega_2 \exp(-\alpha t) \sin \omega_2 t. \quad (18)$$

According to equation (8),  $\Delta F$  can be written as:

$$\Delta F = f(\omega_2) \cos(\omega_2 t + \phi) = f(\omega_2) \cos(\omega_2 t) \cos \phi - f(\omega_2) \sin(\omega_2 t) \sin \phi. \quad (19)$$

By combining eqs. (11), (14), (15), and (19), we obtain

$$m\xi'' = \{cA\omega_2 - f(\omega_2) \sin \phi\} \exp(-\alpha t) \sin \omega_2 t + \{kA + f(\omega_2) \cos \phi\} \exp(-\alpha t) \cos \omega_2 t. \quad (20)$$

The first term on the right side of eq. (20) corresponds to the damping. When  $\phi > 0$ , the coefficient of this term ( $\{cA\omega_2 - f(\omega_2) \sin \phi\}$ ) becomes smaller than  $cA\omega_2$ , since  $\sin \phi$  is positive, which implies that the damping is suppressed by  $\Delta F$ . However, if  $-180 \text{ deg} < \phi < 0 \text{ deg}$ , the damping is enforced by  $\Delta F$ . As shown in Fig. 8, the condition ( $-180 \text{ deg} < \phi < 0 \text{ deg}$ ) is satisfied in our position control system up to 230 Hz. Hence, the measured damping constant becomes higher than that of the ideal conditions.

The ratio  $f(\omega_2)/cA\omega_2$  determines the effect of the positioning force on viscosity. When the sample becomes bigger,  $f(\omega_2)$  increases and  $\omega_2$  decreases, making the ratio larger. The estimated magnitude of  $\Delta F$  was calculated to be between  $10^{-5}$  and  $10^{-6}$  N. This small force has a drastic change upon the measured values. Obviously, this effect is more serious for lower viscosity materials since  $c$  is smaller.

There are several electrostatic levitators around the world which conduct oscillating drop experiments. Even though each levitator has its own characteristics<sup>9,15,21,31,32</sup>, the position control scheme (position detection, electrodes configuration, PID control) is similar. Hence, the results obtained in this research are universal for all these electrostatic levitators.

Precise measurement of the oscillation signal is very significant in this study. As described earlier, our system utilizes a power sensor and a slit. This type of measurement system is utilized by some researchers<sup>9,32</sup>, while others use a high-speed camera combined with image analysis<sup>18</sup>. Since a slit is used, one may think that a large noise will be introduced by the lateral sample translations and would cause a measurement error. The induced error associated with the sample lateral translation can be calculated from geometry. The lateral oscillation of a sample levitated with our facility is within a 100  $\mu\text{m}$  span and exhibits a frequency of around 2 Hz.<sup>23</sup> Assuming a typical sample with a size of 1 mm in radius, the change of the radius due to the lateral translation perpendicular to the axis of observation,  $\varepsilon_l$  can be calculated as:

$$\varepsilon_l = 1 - \cos(\tan^{-1}(100/1000)) = 0.5 \%. \quad (21)$$

In the case that the lateral translation occurs along the axis of observation, an error will be induced due to the changing magnification factor. However, as illustrated in fig.3, the sample shadow is projected to the sensor by a well collimated laser and the lateral motion should not affect the shadow in principle. Similarly, even if the divergence of the laser beam ( $8.7 \times 10^{-3}$  rad; calculated from the specifications of both the laser and the beam expander) is taken into account, the induced error  $\varepsilon_2$  is very small :

$$\varepsilon_2 = 100(\mu\text{m}) \cdot \tan(8.7 \times 10^{-3}) / 2(\text{mm}) = 0.043\% . \quad (22)$$

In our oscillation experiment, the typical deformation of the sample was measured to be  $150\ \mu\text{m}$ , and the ratio to the sample radius  $\varepsilon_3$  was 15 %. Both  $\varepsilon_1$  and  $\varepsilon_2$  are negligible compared with  $\varepsilon_3$ , and the error induced by the lateral sample motion can be neglected in our observation system. The measured raw signals from the oscillation detector in experiment-2 are shown in Figs.12 (a) to (e). If the error induced by the lateral motion is significant, the modulation signal of 2 Hz should be seen in these figures. Apparently, no such signal can be detected, and a FFT analysis did not show any peak around 2 Hz.

Relatively large vertical translations of the sample (as large as the sample radius) are sometimes observed when an excitation signal is superimposed to the top electrode. A typical example is shown in Fig.12 (f). Since the signal profile is completely different from the ones shown in Fig.12 (a) to (e), these data can easily be eliminated from the analysis. In this research, the measured signals were carefully examined and all the data exhibited similar qualities as those shown in Fig.12 (a) to (e). Even though the position control parameters were changed in experiment-2, the position stability was stable and the quality was preserved.

As mentioned before, Hyers pointed out the possible effect of laminar flow inside the levitated sample on the drop oscillation<sup>22</sup>. Although this is not the main cause of the observed phenomenon in experiment-1, this issue remains unsolved. Further research is needed to estimate the magnitude of this effect.

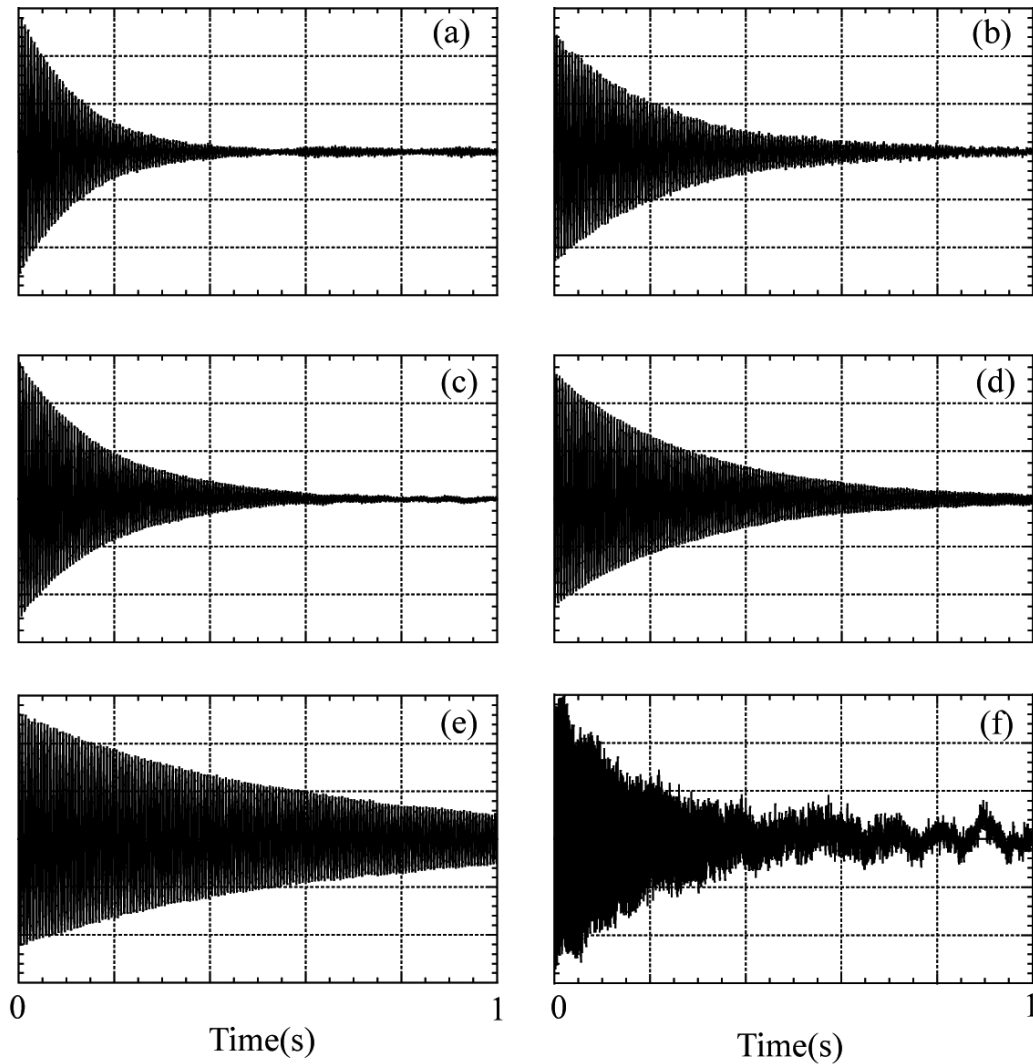


Fig.12 Measured raw signals obtained by the diameter sensing system of Fig.3: (a) experiment 2-1, (b) experiment 2-2, (c) experiment 2-3, (d) experiment 2-4, (e) experiment 2-5, and (f) fluctuated signal due to vertical translation of the sample.

## ACKNOWLEDGMENTS

We are grateful to Dr. S. Adachi (JAXA) for fruitful discussions about the simulation. This research was supported by the Japan Society for the Promotion of Science through their Grant-in-Aid for Science Research (B).

## REFERENCES

- 1) T. Hibiya and I. Egry, *Meas. Sci. Technol.* **16**, 317 (2005).
- 2) B. Glorieux, F. Millot, J.-C. Rifflet and J.-P. Coutures, *Int. J. Thermophys.* **20**, 1085 (1999).
- 3) F. Millot, J. C. Rifflet, V. Sarou-Kanian and G. Wille, *Int. J. Thermophys.* **23**, 1185 (2002).
- 4) T. Richardsen and G. Lohöfer, *Int. J. Thermophys.* **20**, 1029 (1999).
- 5) J. Brillo and I. Egry, *Int. J. Thermophys.* **28**, 1004 (2007).
- 6) H. Kobatake, H. Fukuyama, I. Minato, T. Tsukada, and S. Awaji, *Appl. Phys. Lett.* **90** 94102 (2007).
- 7) S. K. Chung, D. B. Thiessen, and W.-K. Rhim, *Rev. Sci. Instrum.* **67**, 3175 (1996).
- 8) A. J. Rulison and W. -K. Rhim, *Rev. Sci. Instrum.* **65**, 695 (1994).
- 9) W. -K. Rhim, K. Ohsaka, P.-F. Paradis, and E. R Spjut, *Rev. Sci. Instrum.* **70**, 2796 (1999).
- 10) W. -K. Rhim and T. Ishikawa, *Rev. Sci. Instrum.* **69**, 3268 (1998).
- 11) T. Iida and R. I. L. Guthrie, "The Physical Properties of Liquid Metals", Clarendon Press, 1988.
- 12) I. Egry, A. Diefenbach, W. Dreier and J. Piller, *Int. J. Thermophys.* **22**, 569 (2001).
- 13) S. R. Berry, R. W. Hyers, L. M. Racz and B. Abedian, *Int. J. Thermophys.* **26**, 1565 (2005).
- 14) P. -F. Paradis and W. -K. Rhim, *J. Mat. Res.* **14**, 3713 (1999).
- 15) T. Ishikawa, P. -F. Paradis, T. Itami, and S. Yoda, *Meas. Sci. Technol.* **16**, 443 (2005).
- 16) W. -K. Rhim and K. Ohsaka, *J. of Crystal Growth*, **208**, 313 (2000).
- 17) W. -K. Rhim and T. Ishikawa, *Int. J. Thermophys.* **21** 429, (2000).
- 18) R. W. Hyers, R. C. Bradshaw, J. R. Rogers, T. J. Rathz, G. W. Lee, A. K. Gangopadhyay, and K. F. Kelton, *Int. J. Thermophys.* **25**, 1155 (2004).
- 19) G. J. Fan, M. Freels, H. Choo, P. K. Liaw, J. J. Z. Li, W. -K. Rhim, W. L. Johnson, P. Yu, and W. H. Wang, *Applied Physics Letters*, **89**, 241917 (2006).
- 20) T. Ishikawa, J. Yu, and P.-F. Paradis, *Rev. Sci. Instrum.* **77**, 053901 (2006)..
- 21) W. -K. Rhim, S. K. Chung, D. Barber, K. F. Man, G. Gutt, A. Rulison, and R. E. Spjut, *Rev. Sci. Instrum.* **64**, 2961(1993).
- 22) R. W. Hyers, *Meas. Sci. Technol.* **16**, 394 (2005).
- 23) P-F. Paradis, T. Ishikawa, and S. Yoda, *Space Technol.* **3-4**, 81 (2002).
- 24) Lord Rayleigh, *Proc. R. Soc. Lond.* **29**, 71 (1879).
- 25) H. Lamb, *Hydrodynamics*, 6<sup>th</sup> ed., Cambridge University Press, 473 (1932).
- 26) A. D. Agaev, V. I. Kostikov, and V. N. Bobkovskii, *Izv. Akad. Nauk. SSSR Met.* **3**, 43 (1980).
- 27) V. P. Elyutin, M. A. Maurakh, and V. D. Turov, *Izv. Vyssh. Ucheb. Zaved. Chern. Met.* **8** 110,(1965).
- 28) L. Battezzati and A. L. Greer, *Acta metall.* **37**, 1791 (1989).
- 29) T. Itami, in *Condensed Matter Disordered Solids*, edited by S. K. Srivastava and N. H. March (World Scientific, Singapore, 1995), 123-250.
- 30) A. F. D'Souza and Vijay K. Garg, "Advanced Dynamics/ Modeling and Analysis", Prentice-Hall, Inc. (1984).
- 31) A. J. Rulison, J. L. Watkins, and B. Zambrano, *Rev. Sci. Instrum.* **68**, 2856 (1997).
- 32) P. L. Ryder and N. Warncke, in *Solidification and crystallization*, edited by D. M. Herlach (WILEY-VCH Verlag GmbH & Co. KGaA, Weinheim, 2004), 103.
- 33) P.-F. Paradis, T. Ishikawa, N. Koike, Y. Watanabe, *Journal of Rare Earths* **25** (2007), 665.
- 34) P. -F. Paradis, T. Ishikawa and S. Yoda, *Int. J. Thermophys.*, **23**(2002), 825-842.